Journal of Power Sources 207 (2012) 45–50

Contents lists available at SciVerse ScienceDirect

Journal of Power Sources

journal homepage: www.elsevier.com/locate/jpowsour

Short communication

Interpretation of processes at positive and negative electrode by measurement and simulation of impedance spectra. Part II: Concentration limitation☆

Julia Kowal*, Heide Budde-Meiwes, Dirk Uwe Sauer

Electrochemical Energy Conversion and Storage Systems, Institute for Power Electronics and Electrical Drives (ISEA), RWTH Aachen University, Germany

ARTICLE INFO

Article history:
Received 23 September 2011
Accepted 8 December 2011
Available online 17 December 2011

Keywords:
Lead-acid battery
Impedance spectroscopy
Concentration limitation
Kramer-Kronig

ABSTRACT

Impedance measurements of both electrodes of a flooded OEM SLI battery at various SOC and with various direct currents have been measured. For each part of the impedance spectra, an electrochemical process is proposed and implemented in a simulation model. By simulation of impedance spectroscopy, spectra of the model are obtained and compared with the measurement. In the first part, the focus was put on inductive semicircles, while in this second part, concentration limitation and its appearance in impedance spectra is investigated.

1. Introduction

In the first part of this paper, inductive semicircles occurring in the spectra of both positive and negative electrode of lead-acid batteries have been regarded. All spectra shown in that part have been corrected for points that are not consistent according to Kramers–Kronig consistency check.

Strictly speaking, the impedance can only be calculated if three conditions are fulfiled: linearity, time invariance and causality. Minor violations of linearity and time invariance are tolerable, which is then called quasi-linear or quasi-stationary. They can be compensated during the measurement and data processing [4]. If the violations are within tolerable limits can be tested with the Hilbert or Kramers–Kronig transform [1,6,7]. Especially non-linearity is not a problem if both real and imaginary part changes by the same factor [7]. The principle of Kramers–Kronig is to calculate the real part from the imaginary part or vice versa:

$$\mathrm{Im}\{\underline{Z}(\omega)\} = \frac{2\omega}{\pi}\int_0^{\infty}\frac{\mathrm{Re}\{\underline{Z}(\nu)\} - \mathrm{Re}\{\underline{Z}(\omega)\}}{\nu^2-\omega^2}d\nu \quad (1)$$

$$\mathrm{Re}\{\underline{Z}(\omega)\} = Re\{\underline{Z}(\omega\to\infty)\} + \frac{2\omega}{\pi}\int_0^{\infty}\frac{\nu\cdot\mathrm{Im}\{\underline{Z}(\nu)\} - \omega\cdot\mathrm{Im}\{\underline{Z}(\omega)\}}{\nu^2-\omega^2}d\nu \quad (2)$$

The calculation can then be compared with the measurement. From Eqs. (1) and (2) it becomes clear that also measurements at $\omega = 0$ and $\omega\to\infty$ are needed to calculate the integrals. Schiller et al. [3] have developed a method called Z-HIT to overcome this problem. The absolute value of the impedance $|\underline{Z}|$ is estimated from the phase angle ϕ taking into account the frequency range from starting frequency ω_s to the currently regarded frequency ω:

$$\ln\left(\frac{|\underline{Z}(\omega)|}{|\underline{Z}(0)|}\right) = \frac{2}{\pi}\int_{\omega_s}^{\omega}\phi(\nu)d\ \ln\ \nu + \sum_{k\geq 1,k\ \mathrm{odd}}\gamma_k\frac{d^k\phi(\omega)}{(d\ \ln\ \omega)^k} \quad (3)$$

The first term on the right hand side is the logarithmic Hilbert transform and the second term is a correction term accounting for the limited frequency range.

Now, also the points that are not consistent are considered. Simulations assuming concentration limitation as the origin for the deformation are shown and compared with the measurements.

2. Impedance spectra of lead-acid battery electrode

The impedance spectra of the positive and negative electrode shown in Figs. 1 and 2 [Part I of this paper] are corrected for impedance values that did not pass the Kramers–Kronig consistency check, indicating that at least one prerequisite (linearity, stationarity, causality) was not fulfiled. Figs. 3 and 4 show the same spectra as Figs. 1 and 2, respectively, but including those values. Both at the negative and the positive electrode, the consistency check fails at low frequencies at the end of each measurement.

☆ This paper was presented at 8th international LABAT conference 2011 in Albena, Bulgaria.

* Corresponding author. Tel.: +49 241 8096935; fax: +49 241 8092203.
E-mail addresses: batteries@isea.rwth-aachen.de, sf@isea.rwth-aachen.de (J. Kowal).

0378-7753/$ – see front matter © 2011 Elsevier B.V. All rights reserved.
doi:10.1016/j.jpowsour.2011.12.014

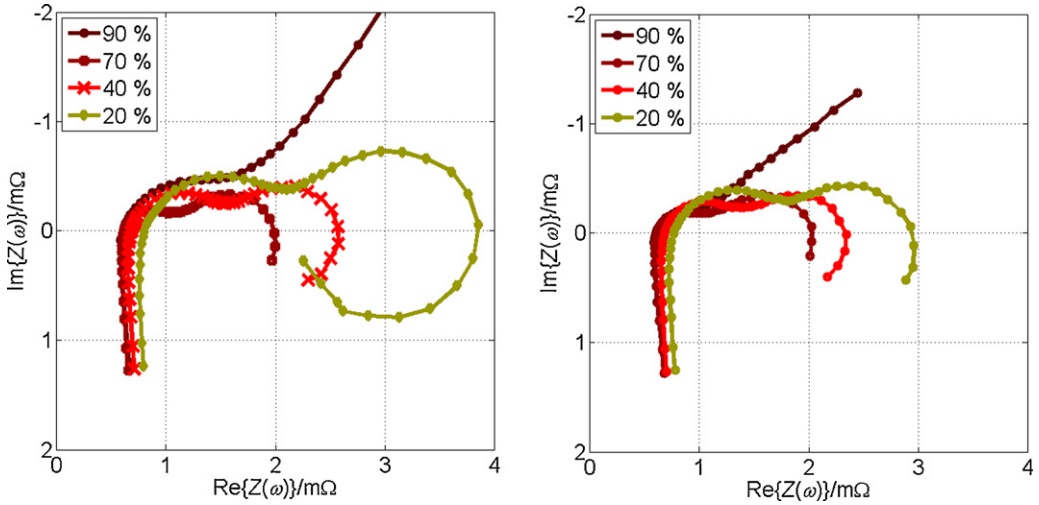

Fig. 1. Impedance spectra during charging (left) and discharging (right) of the negative electrode of a 60 Ah flooded lead-acid battery at different SOC at 25 °C, superposed direct current is ±0.5 I_{20} and the SOC was adjusted by discharging. Measured frequencies are between 6 kHz and 3 mHz with eight frequencies per decade. Points that do not pass Kramers–Kronig consistency check are not shown; the complete spectra are depicted in Fig. 3.

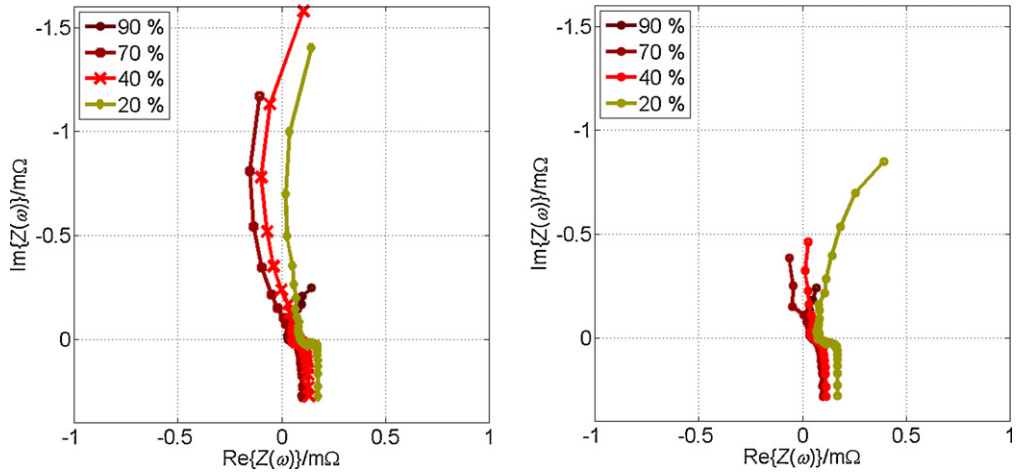

Fig. 2. Impedance spectra during charging (left) and discharging (right) of the positive electrode of a 60 Ah flooded lead-acid battery at different SOC at 25 °C, superposed direct current is ±0.5 I_{20}. The SOC was adjusted by discharging. Measured frequencies are between 6 kHz and 3 mHz with eight frequencies per decade. Points that do not pass Kramers–Kronig consistency check are not shown; the complete spectra are depicted in Fig. 4.

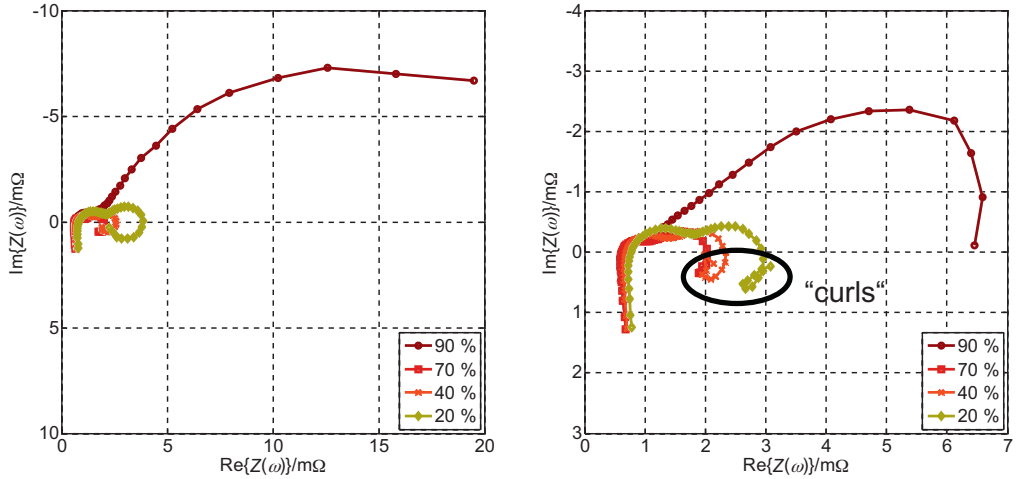

Fig. 3. Impedance spectra of the negative electrode during charging (left) and discharging (right) as in Fig. 1 (different SOCs at 25 °C, superposed direct current is ±0.5 I_{20}), but including impedance values that do not pass Kramers–Kronig consistency check. Note the different scaling. Measured frequencies are between 6 kHz and 3 mHz with eight frequencies per decade [2].

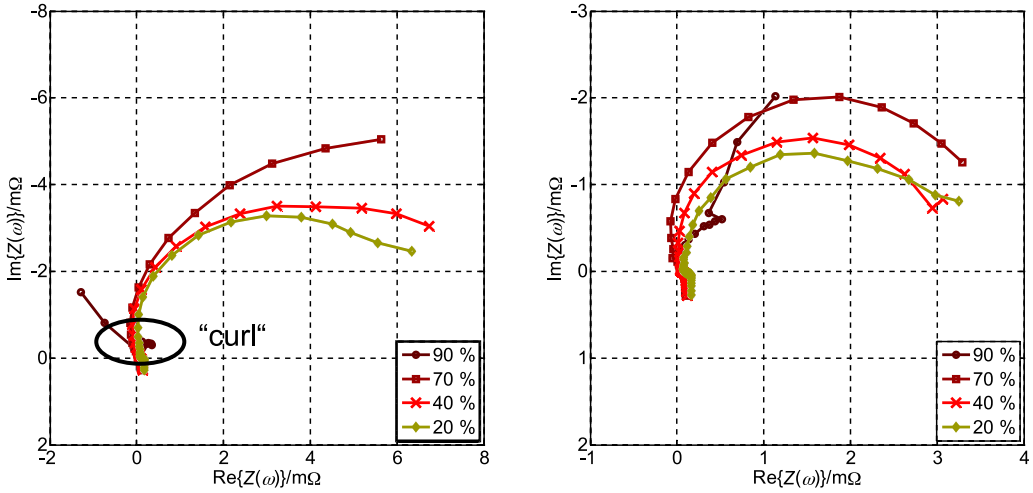

Fig. 4. Impedance spectra of the positive electrode during charging (left) and discharging (right) as in Fig. 2 (different SOCs at 25 °C, superposed direct current is ±0.5 I_{20}), but including impedance values that do not pass Kramers–Kronig consistency check. Note the different scaling. Measured frequencies are between 6 kHz and 3 mHz with eight frequencies per decade [2].

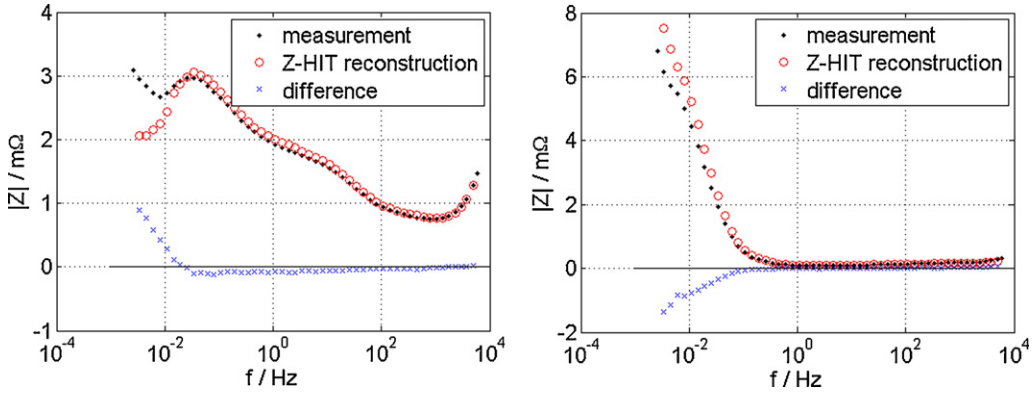

Fig. 5. Measured and calculated (Z-HIT reconstruction) absolute value of the impedance left: negative electrode at 20% SOC during discharge with 0.5 I_{20} (corresponding to Fig. 3 right), right: positive electrode at 20% SOC during charge with 0.5 I_{20} (corresponding to Fig. 4 left).

Fig. 5 exemplarily shows a comparison between the measured and reconstructed absolute value of the impedance for selected spectra of the positive and negative electrode. At the negative electrode, the agreement is quite good down to a frequency of about 20 mHz and only down to about 100 mHz at the positive electrode.

A failure of the consistency check does not necessarily mean that the measurement equipment does not work well. As the problem always arises at low frequencies, it is more likely that the battery leaves the tolerable range of deviation from linearity, stationarity and causality after some time of constant current charging or discharging. Consequently, the prerequisites for the Kramers–Kronig transform are not fulfiled at the corresponding frequencies.

Most probably, the concentration limitation of the reaction partners Pb^{2+} and SO_4^{2-} ions leads to instationary and acausal behaviour of the battery. Concentration influences charge transfer in a way that small concentration leads to a large charge-transfer impedance. At the negative electrode, concentration limitation additionally leads to "curls" at lower states of charge (Fig. 3 right) and at the positive electrode at 90% SOC also a kind of curl can be observed (Fig. 4 left) and the real part of the impedance becomes negative in some cases. Even though the remaining points passed Kramers–Kronig check, this does not mean that they are not influenced by concentration limitation. Especially the values close to those left out are most probably also influenced by concentration, but the variation from one measurement to the next is so small that the measurement can be assumed to be quasi-stationary.

3. Simulation

In the first part of this paper, concentration limitation has been neglected. In reality, especially at low frequencies, the limitation of charge carriers can be observed from curls or large impedance values at low frequencies. Instationarities can occur at both electrodes and both during charging and discharging, which means that a limitation of both Pb^{2+} ions during charging (reverse reaction of step 2 in Fig. 6) and of SO_4^{2-} ions during discharging (step 3 in Fig. 6). Such behaviour can also be simulated by limiting the concentration. For this, frequency-dependent factors are introduced in the differential equations of the negative (Section 3.1) and the positive (Section 3.2) electrode.[1] Equations to describe the concentration of Pb^{2+} ions and H_2SO_4 have been derived by Sauer and simplified by

[1] In reality, the concentration is not frequency dependent. However, as the concentration falls or rises with proceeding charge or discharge, this leads to an apparent frequency dependency in a spectrum with superposed direct current. For simplicity, in the simulations the concentration is kept constant for each frequency, while in reality it changes gradually all the time.

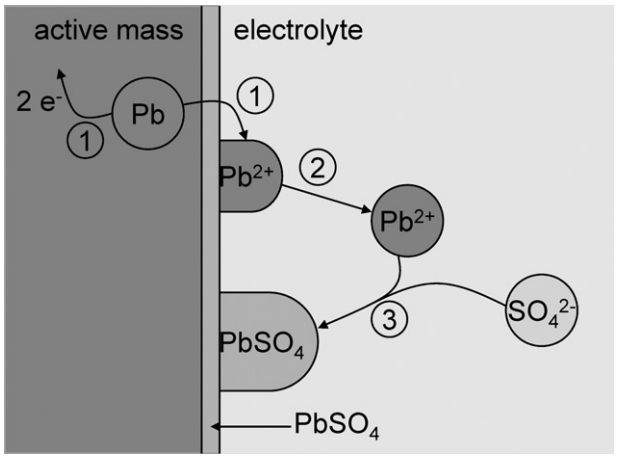

Fig. 6. Course of reaction during discharge (see Part I of this paper): (1) charge transfer, (2) desorption, and (3) chemical reaction.

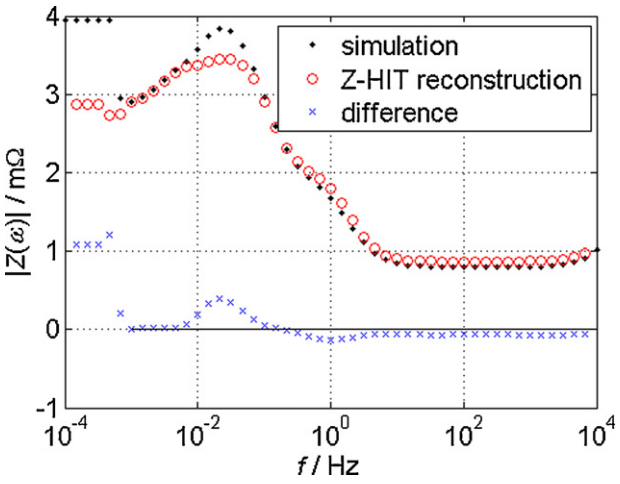

Fig. 8. Kramers–Kronig consistency check (Z-HIT) for the simulation with 4 I_{20} in Fig. 7.

Thele [5]. They are further simplified in the following as the aim here is only to demonstrate the general impact of concentration limitation.

A failure in Kramers–Kronig consistency check (Z-HIT) does not necessarily indicate a failure of the measurement device, but simply that at least one of the prerequisites linearity, causality and stationarity is violated. The simulations shown in the following indicate that concentration limitation leads to a failure in the consistency check, so it can be assumed that this is also what happens during the measurements. A concentration variation with frequency violates at least the demand for stationarity. Stationarity requires that no other parameter than frequency changes from one measurement to another. Also causality is not fulfiled because the impedance is not only influenced by the input parameters current and voltage, but also by concentration, which cannot be influenced from outside.

3.1. Negative electrode

Concentration factors $c_{H_2SO_4}(f)/c^0_{H_2SO_4}$ and $c_{Pb^{2+}}(f)/c^0_{Pb^{2+}}$ are added in the adsorption/desorption part of the coverage equation of the negative electrode (cp. Eq. (5) in Part I of this paper):

$$\frac{d\theta(t)}{dt} = k_{ct}\cdot\left((1-\theta(t))\cdot\exp\left(\frac{\alpha nF}{RT}\eta(t)\right) - \theta(t)\cdot\exp\left(-\frac{(1-\alpha)nF}{RT}\eta(t)\right)\right) - k_{desad}\cdot\begin{pmatrix}(c_{H_2SO_4}(f))/(c^0_{H_2SO_4})\cdot\theta(t)\cdot\exp((\beta nF/RT)\eta(t))\\ -(c_{Pb^{2+}}(f)/c^0_{Pb^{2+}})\cdot(1-\theta(t))\cdot\exp(((1-\beta)nF/RT)\eta(t))\end{pmatrix} \quad (4)$$

A simplified equation to calculate the H_2SO_4 concentration in the pores of the negative electrode is:

$$c_{H_2SO_4}(t) = \frac{1}{\varepsilon_{neg}(t)}\int \varepsilon^{ex}_{neg}(t)\cdot D_{H_2SO_4}(c_{H_2SO_4})\cdot\frac{\Delta c_{H_2SO_4}(t)}{\Delta x^2} + G_{MR,neg} + G_{SR,neg}dt \quad (5)$$

ε_{neg} is the porosity of the negative electrode, *ex* is an exponent, $D_{H_2SO_4}$ is the diffusion parameter of sulphuric acid, Δx is the diffusion distance and G_{MR} and G_{SR} are generation/consumption terms for main and side reactions. During impedance-spectroscopy simulation it is assumed that the SOC and thus porosity stays more or less constant. Gassing is not considered in the model and it can also be assumed that the diffusion parameter stays constant. Thus, for a rough estimation of the concentration, assuming further that the concentration is constant during the simulation of each frequency f_i, Eq. (5) simplifies to:

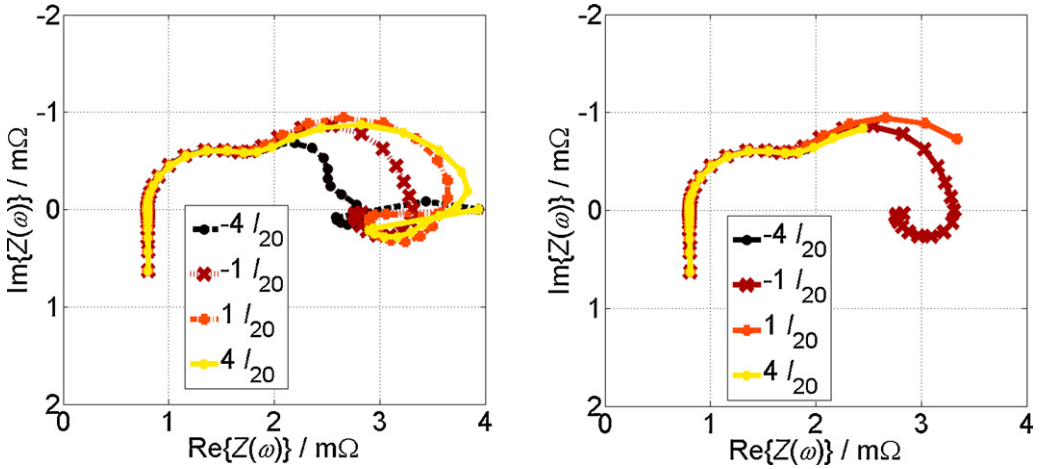

Fig. 7. Simulation of negative electrode with frequency-dependent concentration limitation, frequency range 10 kHz to 0.1 mHz, eight frequencies per decade, with $R_0 = 0.8\,m\Omega$, $R_{coating} = 1\,m\Omega$, $C_{coating} = 100\,F$, $\alpha = 0.6$, $\beta = 0.5$, $i_0 = 15\,A$, $C_{DL} = 1000\,F$, $k_{ct} = 0.001\,s^{-1}$ and $k_{desad} = 0.005\,s^{-1}$, left: original, right: after removal of points that fail Kramers–Kronig consistency check (Z-HIT).

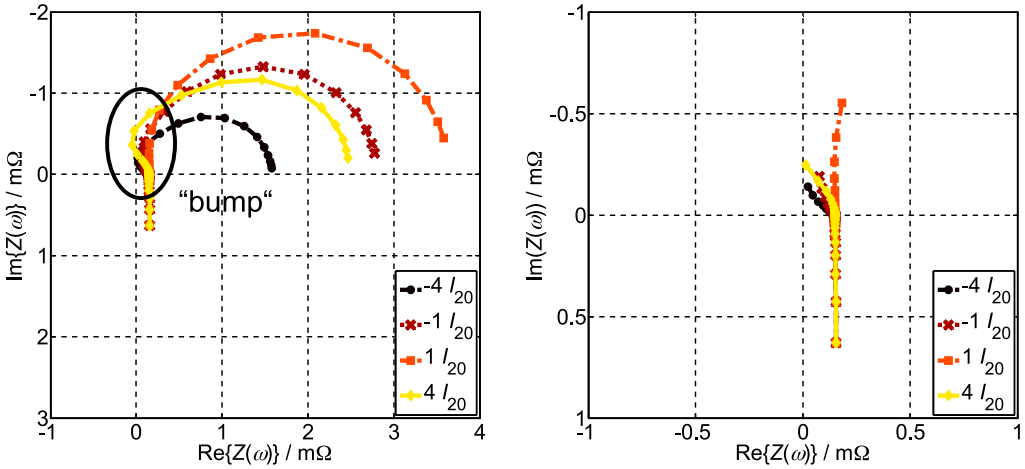

Fig. 9. Simulations of positive electrode with frequency-dependent concentration limitation, frequency range 10 kHz to 1 mHz, eight frequencies per decade, with $R_0 = 0.1\ \mathrm{m\Omega}$, $C_{DL} = 5000\ \mathrm{F}$, $\alpha = 0.4$, $I_0 = 2\ \mathrm{A}$; left: original, right: after removal of points that fail Kramers–Kronig consistency check (Z-HIT).

$$c_{H_2SO_4}(f_i) = c_{H_2SO_4}(f_{i-1}) + \frac{\varepsilon_{neg}^{ex} \cdot D_{H_2SO_4} \cdot ((c_{H_2SO_4}(f_{i-1}) - c^0_{H_2SO_4})/\Delta x^2) + G_{MR,neg}}{\varepsilon_{neg}} \Delta t \quad (6)$$

With $G_{MR} = I \cdot (2\,t_0^+ - 1)/2F$ and dividing by the equilibrium concentration $c^0_{H_2SO_4}$ this becomes:

$$\frac{c_{H_2SO_4}(f_i)}{c^0_{H_2SO_4}} = \frac{c_{H_2SO_4}(f_{i-1})}{c^0_{H_2SO_4}} + \frac{\varepsilon_{neg}^{ex} \cdot (D_{H_2SO_4}/\Delta x^2) \cdot ((c_{H_2SO_4}(f_{i-1})/c^0_{H_2SO_4}) - 1) + (1/c^0_{H_2SO_4}) \cdot (((2t_0^+ - 1) \cdot I)/2F)}{\varepsilon_{neg}} \Delta t \quad (7)$$

For $i = 1$, $c_{H_2SO_4}(f_{i-1})/c^0_{H_2SO_4} = 1$ is assumed.

The concentration of the Pb^{2+} ions can be calculated from:

$$\frac{dc_{Pb^{2+}}(t)}{dt} = q - s \quad (8)$$

$q = -I/(2FV_{uni})$ is the amount of ions generated or consumed by the main reaction; the negative sign is needed because charging consumes ions and discharging generates them. V_{uni} is a unified volume. s is the amount of Pb^{2+} ions that combines with SO_4^{2-} ions to lead sulphate. It depends on the radius distribution $f(r,t)$ of the existing sulphate crystals:

$$s = \frac{4\pi}{3} \cdot \frac{1}{v_m} \cdot \frac{d}{dt} \int_{r*}^{\infty} r^3 \cdot f(r,t)dr \quad (9)$$

Eq. (9) can be simplified for the case that all crystals have the same radius. This simplification is good enough for a rough estimation of the concentration:

$$s = 4 \cdot \pi \cdot N \cdot r \cdot D_{Pb^{2+}} \cdot (c_{Pb^{2+}} - c^0_{Pb^{2+}}) \quad (10)$$

Assuming again that the concentration is constant for each frequency Eq. (8) becomes:

$$\frac{c_{Pb^{2+}}(f_i)}{c^0_{Pb^{2+}}} = \frac{c_{Pb^{2+}}(f_{i-1})}{c^0_{Pb^{2+}}} - \left(\frac{1}{c^0_{Pb^{2+}}} \cdot \frac{I}{2F \cdot V_{uni}} + 4 \cdot \pi \cdot N \cdot r \cdot D_{Pb^{2+}} \cdot \left(\frac{c_{Pb^{2+}}(f_{i-1})}{c^0_{Pb^{2+}}} - 1 \right) \right) \cdot \Delta t \quad (11)$$

Fig. 7 left shows simulated spectra with concentration limitation. In analogy to the measurements, high frequencies are simulated first so that limitation becomes only visible at low frequencies. As in the measurements, curls occur at low frequencies. Fig. 8 shows a comparison of the simulated and the reconstructed absolute value of the impedance corresponding to the spectrum at $4\,I_{20}$ in Fig. 7 left. Fig. 7 right shows the simulated spectra after removing the values that did not pass Kramers–Kronig consistency check. Apart from the $-1\,I_{20}$ simulation, no inductive semicircle is visible any more, which makes it practically impossible to identify the corresponding parameters. Comparison with the corresponding simulation without concentration limitation [Part I of this paper] shows that the remaining values are still partly influenced by the limited concentration.

3.2. Positive electrode

Neglecting the high-frequency inductive semicircle and assuming that no adsorption/desorption process occurs, the faradaic impedance of the positive electrode simply consists of a charge-transfer resistance. The overall impedance is then a purely ohmic resistance in parallel to the double layer capacitance plus an additional series inductance L. However, the Kramers–Kronig consistency check of the measured spectra (Fig. 5) suggests that strong concentration limitation is present. Similar to the negative electrode, frequency-dependent concentration factors can be added; here to the Butler–Volmer equation:

$$i_{ct,pos} = i_0 \cdot \left(\frac{c_{Pb^{2+}}(f)}{c^0_{Pb^{2+}}} \cdot \exp\left(\frac{\alpha \cdot n \cdot F}{R \cdot T} \cdot \eta \right) - \frac{c_{H_2SO_4}(f)}{c^0_{H_2SO_4}} \cdot \exp\left(-\frac{(1-\alpha) \cdot n \cdot F}{R \cdot T} \cdot \eta \right) \right) \quad (12)$$

The factors are calculated analogously to Eqs. (7) and (11), but with the corresponding values for the positive electrode for porosity and diffusion distance Δx. The generation term of the main reaction G_{MR} is different as well:

$$G_{MR,pos} = \frac{(3 - 2t_0^+) \cdot I}{2F} \quad (13)$$

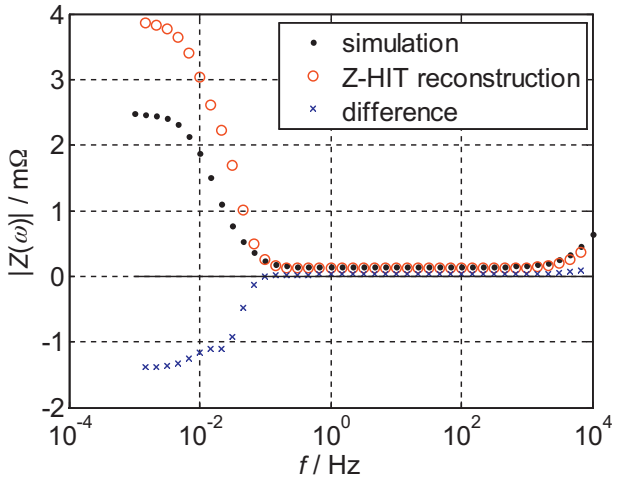

Fig. 10. Kramers–Kronig consistency check (Z-HIT) for simulation with 4 I_{20} in Fig. 9.

Fig. 9 left shows simulated spectra of a positive electrode with concentration limitation. Similar to the measurements, the semicircle shows a "bump" and the real part even becomes negative at some currents. Fig. 9 right shows the same simulation leaving out the points that do not pass Kramers–Kronig consistency check (Fig. 10). As for the measurements (Fig. 2), not much of the spectrum is left and it is hard to extract impedance parameters from this. Also, it can be seen that even though the remaining impedance values pass the consistency check, they are still affected by the concentration limitation, indicated by the bend toward the imaginary axis.

4. Conclusion

Deformations of the spectra of both electrodes of lead-acid batteries due to concentration limitation have been discussed. It has been demonstrated that a frequency-dependent concentration of Pb^{2+} ions and H_2SO_4 leads to curls in the spectra of the negative electrode at low frequencies and to bumps in the capacitive semicircle of the positive electrode at intermediate frequencies, similar to the measured spectra. Also, Kramers–Kronig transform fails for those frequency ranges, just as for the measurements. It is thus very likely that concentration limitation is the cause for stationarity violations and consequent deformations of the spectra.

Acknowledgements

This work was kindly financed by the E.ON International Research Initiative within the project BEST. The authors would like to thank Dr. Eckhard Karden from Ford Research and Advanced Engineering Europe, Aachen, Germany, for valuable discussion.

References

[1] B.A. Boukamp, Impedance spectroscopy, strength and limitations (Impedanzspektroskopie, Stärken und Grenzen), Technisches Messen 71 (2004) 509–518.
[2] H. Budde-Meiwes, J. Kowal, D.U. Sauer, E. Karden, How can impedance spectroscopy be trusted? A review on quality, to be presented at 12th European Lead Acid Battery Conference (ELBC) in Istanbul, September 21–24, 2010 and to be submitted to J. Power Sources.
[3] C.A. Schiller, F. Richter, E. Gülzow, N. Wagner, Validation and evaluation of electrochemical impedance spectra of systems with states that change with time, Phys. Chem. Chem. Phys. 3 (2001) 374–378.
[4] C.A. Schiller, W. Strunz, Impedanzmessungen an Systemen mit merklicher zeitlicher Drift, in: Technische Mitteilungen, vol. 99, 1. Symposium Impedanzspektroskopie, Haus der Technik, Essen, May 2006, pp. 107–111. ISSN 0040-1439.
[5] M. Thele, A contribution to the modelling of the charge acceptance of lead-acid batteries – using frequency and time domain based concepts, PhD thesis, RWTH Aachen University, Institute for Power Electronics and Electrical Drives ISEA, 2007.
[6] M. Urquidi-Macdonald, S. Real, D.D. Macdonald, Application of Kramers–Kronig transforms in the analysis of electrochemical impedance data – II. Tranformations in the complex plane, J. Electrochem. Soc. 133 (1986) 2018–2024.
[7] M. Urquidi-Macdonald, S. Real, D.D. Macdonald, Applications of Kramers–Kronig transforms in the analysis of electrochemical impedance data – III. Stability and linearity, Electrochim. Acta 35 (1990) 1559–1566.